Journal of Marine Science and Technology

Volume 29 | Issue 6 Article 7

Long-term variation of sea surface temperature in relation to sea level pressure and surface wind speed in southern Indian Ocean

Sandipan Mondal
National Taiwan Ocean University, Keelung, Taiwan, ROC

Ming-An Lee
National Taiwan Ocean University, Keelung, Taiwan, ROC, malee@mail.ntou.edu.tw

Yi-Chen Wang
National Taiwan Ocean University, Keelung, Taiwan, ROC

Bambang Semedi
Brawijaya University, Malang, East Java, Indonesia

RESEARCH ARTICLE

Long-term Variation of Sea Surface Temperature in Relation to Sea Level Pressure and Surface Wind Speed in Southern Indian Ocean

Sandipan Mondal [a], Ming-An Lee [a,b,*], Yi-Chen Wang [a], Bambang Semedi [c]

[a] Department of Environmental Biology and Fisheries Science, National Taiwan Ocean University, Keelung 202, Taiwan, ROC
[b] Center of Excellence for Ocean Engineering, National Taiwan Ocean University, Keelung, Taiwan, ROC
[c] Fisheries and Marine Science Faculty, Brawijaya University, Malang, East Java, Indonesia

Abstract

Sea surface temperature (SST) is an essential parameter associated with fish habitat and changes in oceanic conditions. Long-term SST variation in relation to sea level pressure (SLP) and surface wind speed (SWS) was observed based on the National Oceanic and Atmospheric Administration (NOAA) data of southern Indian Ocean. Mean monthly time series showed that February and November were the warmest and coolest months, respectively. Spatial distribution showed that 0°S−30°S was warm with SST of 20°−30 °C, which was higher than that at all other places throughout the year. SLP (>1010 millibar) and SWS (>12 m/s) were high at 20°S−40°S and 45°S−50°S, respectively. SST was strongly negatively correlated with SWS but strongly positively correlated with SLP. Long-term yearly time series of SST showed that 2016 and 1948 were the warmest and coolest years, respectively, during the study period. Decadal time series showed that 1978−1987 had the highest decadal change. SST anomalies were almost negative before 1970, positive after 1970, high after 2008, and the highest in 2016. Southwest Indian Ocean was warmer than southeast Indian Ocean in summer and vice versa in winter. SST changes during 1948−2018 were higher than those during 1948−1972 and 1973−2018 for all the 4 months.

Keywords: Sea surface temperature, Subtropical Indian ocean dipole, Surface level pressure, Surface wind speed and southern Indian ocean

1. Introduction

Sea surface temperature (SST) is defined as water temperature close to the ocean's surface. The exact meaning of the surface depends on the measurement method, but generally, it is between 1 mm (0.04 in) and 20 m (70 feet) below the sea surface. Air masses in the Earth's atmosphere within a short distance from the shore are highly affected by SSTs. Warm SSTs cause tropical cyclogenesis over the Earth's oceans. Tropical cyclones can cause a cool wake due to turbulent mixing of the upper 30 m (100 feet) of the ocean. SST changes diurnally, like the air above it, but to a lesser degree. SST variation is lower on breezy days than on calm days. In addition, ocean currents, such as the Atlantic Multi-decadal Oscillation, can affect SSTs on multidecadal time scales [1], and the global thermohaline circulation has a major impact and affects average SST significantly throughout most of the world's oceans. Climate and weather are largely influenced by SST. El Niño causes changes in rainfall patterns around the globe, causing heavy rainfall in the southern United States and severe drought in Australia, Indonesia, and southern Asia, and it can be hallmarked by sea surface warming. On a small scale, ocean temperatures influence the development of tropical cyclones (hurricanes and

Received 21 May 2020; revised 30 June 2020; accepted 7 September 2020.
Available online 27 December 2021

* Corresponding author at: Department of Environmental Biology and Fisheries Science, National Taiwan Ocean University, Keelung 202, Taiwan, ROC.
E-mail address: malee@mail.ntou.edu.tw (M.-A. Lee).

https://doi.org/10.514/2709-6998.2558

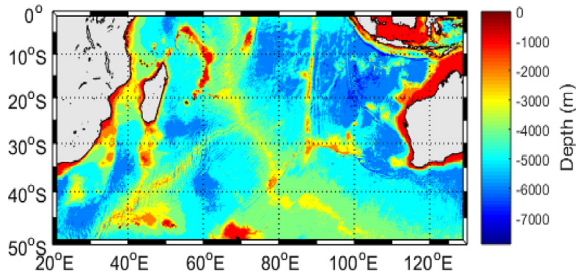

Fig. 1. Bathymetry of the study area.

typhoons), which draw energy from warm ocean waters to form and intensify [2].

Climate change is one of the major stressors that affects fishery globally. Therefore, observing the climatological patterns of different environmental factors is crucial. SST is essential to understand the global climate. SST is a crucial indicator of the state of the Earth's climate system. Thus, appropriate assessment of SST is essential for climate monitoring, research, and prediction [3]. SST variations control meteorological and oceanographic processes such as change in current speed or the frequency of events including El Nino, monsoon depressions, subsequent floods, large-scale sea level fluctuations, and formation of tropical cyclones. Furthermore, the expected rise in SST of approximately 0.2°C-2.5 °C [4] may cause sea level rise and other natural disasters, such as an increase in storm frequency and intensity and sea water encroachment into agricultural land [5,6]. The rise in SST increases the saturation of vapor pressure, which triggers the formation of water vapors and latent heat, causing cyclone intensification. Evan and Camargo [7] and Emanuel [8] have explained the significance of SST in increasing cyclonic intensity in addition to floods and other natural disasters. Observations indicate the existence of a temperature threshold necessary for the development of major hurricanes rather than a continuous positive relationship between maximum storm intensity and SST [9]. Moreover, the southern Indian Ocean (SIO) is one of the best fishing zones for commercial fishes such as tuna. Therefore, careful monitoring of SST is required to assess its impacts on the regional weather and climate system as well as consequent effects on the socioeconomic system. This study analyzed the long-term temporal and spatial changes in SST in the SIO to understand the changes in the marine environment (see Fig. 1).

2. Materials and methods

2.1. Remote sensing data

The SST dataset used in this study is the global SST dataset maintained by the Met Office Hadley Centre, UK. In addition to SST, data used in the present study were (1) sea level pressure (SLP), (2) U-wind, (3) V-wind, and (4) surface wind speed (SWS). All the data were collected for the period of 1948−2018. The source of data along with the spatial resolution is shown in Table 1. SWS data were used to estimate the wind velocity without considering the direction. U-wind and V-wind datasets were used to determine the wind direction. Following the methodology of Prajapati et al. [10]; datasets were smoothly interpolated with the bipolar interpolation algorithm by using MATLAB software version 2015a. All the data were area-weight averaged to obtain the individual monthly SST, SLP, and SWS, and these individual monthly values were further averaged to obtain the annual mean of SST, SLP, and SWS.

2.2. Data analysis

February, May, August, and November were designated as the representative months for summer, autumn, winter, and spring, respectively. Therefore, the monthly climatological patterns and seasonal changes over only these 4 months were determined.

2.2.1. Monthly and yearly variations

Time series analysis is one of the most valuable tools for investigating fluctuations in both long- and short-term values. To determine monthly variation in climatic trends across the SIO, the mean monthly time series of SST, SLP, and SWS were extracted through time series analysis. Furthermore, the standard deviation of monthly changes was calculated in the analysis to better understand the

Table 1. Sources of different satellite-derived data

Data	Unit	Source	Website	Spatial Resolution
SST	°C	HadISST_sst.nc	https://coastwatch.pfeg.noaa.gov/erddap/griddap/erdHadISST.html	1° × 1°
SLP	millibar	pres.mon.mean.nc	https://psl.noaa.gov/data/gridded/data.ncep.reanalysis.surface.html	2.5° × 2.5°
U	m/sec	uwnd.mon.mean.nc	https://psl.noaa.gov/data/gridded/data.ncep.reanalysis.surface.html	2.5° × 2.5°
V	m/sec	vwnd.mon.mean.nc	https://psl.noaa.gov/data/gridded/data.ncep.reanalysis.surface.html	2.5° × 2.5°
SWS	m/sec	wspd.mon.mean.nc	https://psl.noaa.gov/data/gridded/data.ncep.reanalysis.surface.html	2.5° × 2.5°

monthly changes in SST, SLP, and SWS. The relations between SST and SWS, SST and SLP, and SLP and SWS were examined using the monthly mean data through the Pearson correlation coefficient test with SPSS software version 22. Monthly changes in the climatological pattern were observed using ArcGIS software version 10.4. Moreover, variations in the yearly and decadal SST were examined through time series analysis, and standard deviation of SST changes in every year and decade was estimated. Long-term monthly and yearly variations were examined, and a figure was extracted through the bipolar interpolation algorithm by using MATLAB software version 2015a. The SST anomaly changes during 1948–2018 were examined to check monthly and yearly changes. To clarify the relationship between the SST and different environmental factors, a two-tailed Pearson correlation analysis was performed using SPSS (version 22.0).

2.2.2. Tempo-spatial and seasonal variations

The data of 1948–1972, 1972–2018, and 1948–2018 were compared to better understand the tempo-spatial warming trend during the study period. Figures for tempo-spatial changes were extracted through the bipolar interpolation algorithm by using MATLAB software version 2015a. As February, May, August, and November were designated as the representative months for summer, autumn, winter, and spring, respectively, seasonal changes over only these 4 months were investigated. Seasonal SST changes during 1948–1972, 1973–2018, and 1948–2018 were compared to determine the warming trend. Figures were extracted using the same procedure as tempo-spatial changes.

3. Results

3.1. Mean monthly variations in SST, SLP, and SWS

3.1.1. Time series analysis

The mean monthly changes in SST, SLP, and SWS were examined using the time series analysis. Fig. 2a indicates that February and August were the warmest and coolest months during 1948–2018, with an SST of 21.42 °C and 18.14 °C, respectively. Standard deviation of SST from January to December was 2.43 °C. The mean highest and lowest SLP occurred in January and October, with a mean value of 965.01 and 963.55 millibar, respectively. A standard deviation of 0.89 millibar was observed for SLP from January to December (Fig. 2b). The mean highest and lowest SWSs were observed in July and March, with mean values of 7.95 m/s and 6.35 m/s, respectively (Fig. 2c). A standard deviation of 1.29 m/s was observed for SWS from January to December. Monthly mean is given instead of every month in every year due to missing data in some months.

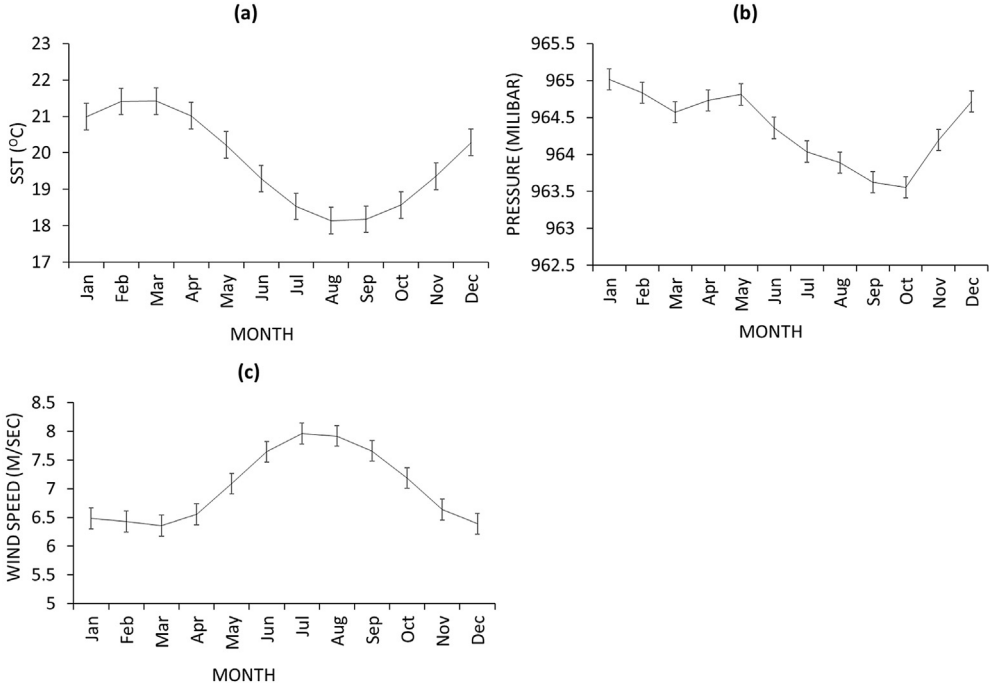

Fig. 2. Time series of mean monthly changes in (a) SST, (b) SLP, and (c) SWS during 1948–2018 by using standard deviation.

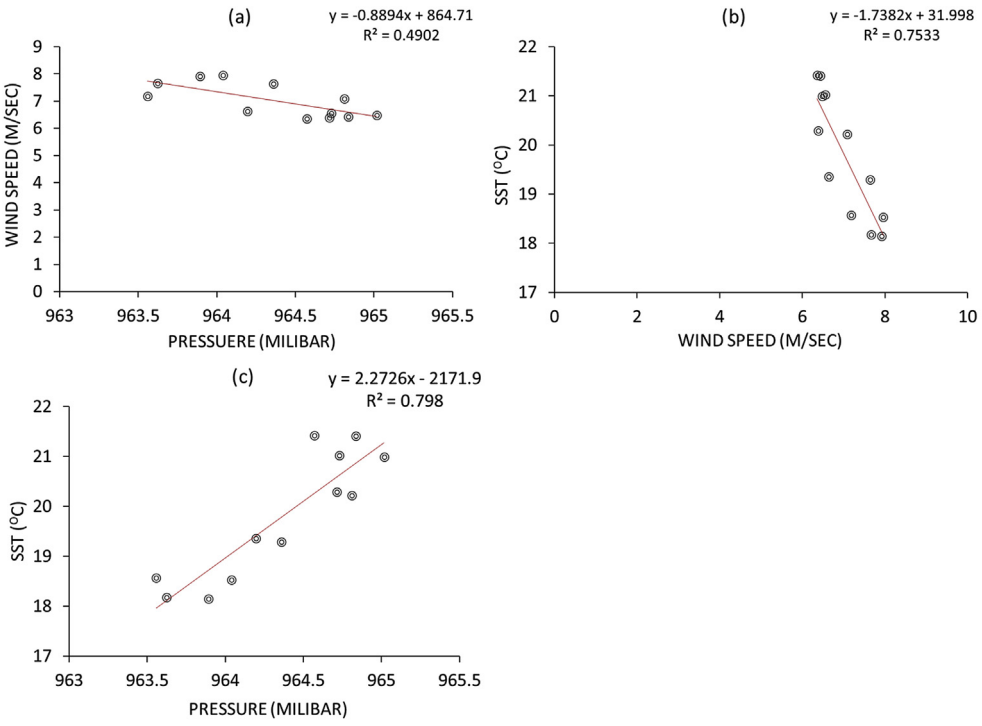

Fig. 3. Pearson correlation coefficient test of (a) SST vs SLP, (b) SST vs SWS, and (c) SWS vs SLP.

3.1.2. Relation between SST, SLP, and SWS

Associations between SST and SWS, SST and SLP, and SLP and SWS were evaluated using the Pearson correlation coefficient method. The monthly means of SST, SLP, and SWS were used to determine the relation intensity among the parameters. "R" indicates the correlation value. SST was strongly positively correlated with SLP (Fig. 3a) but strongly negatively correlated with SWS (Fig. 3b). SWS and SLP (Fig. 3c) were strongly negatively correlated, with a value of −0.7 (approx.). R values between different parameters are shown in Table 2.

3.1.3. Climatological patterns of SST, SLP, and SWS

The SST range at 40°S–50°S was 15°–20 °C in all the 4 months (Fig. 4a). Cool water started shifting toward the north from May to November. The 10 °C and 15 °C isotherm lines were near 45°S and 40°S, respectively, throughout the year. The 20 °C isotherm line was at 40°S during February, which started shifting toward the north and reached near 30°S by November. The area between 0° and 30°S had >25 °C SST throughout the year. The 25 °C isotherm line was detected at 30°S during February, and similar to the 20 °C isotherm, it started shifting toward the north after February. In August, this 25 °C isotherm line was near 10°S, and it crossed 10°S between 40°E and 80°E. In November, the 25 °C isotherm line started shifting in the opposite direction and was at 25°S. During February, 30°S–40°S had an SLP between 1015 and 1020 millibar, and the rest of the study area except the coastal areas had an SLP of 1010–1014 millibar (Fig. 4b). Coastal areas had a lower SLP of approximately 1000 millibar. In May and August, high SLP zones were observed between 10°S and 40°S. During May, some places (50°E, 60°E, 70°E, and 80°E) near 30°S showed a high SLP value such as 1025 millibar. This high SLP zone extended up to 20°S–35°S and 35°E–95°E in August. The condition of November was almost the same as that of February. The area near 50°S showed an SLP range of 1000–1005 millibar in all the 4 months. SWS was <5 m/s in the area between 0°S and 20°S in February, and the wind direction was mainly eastward (Fig. 4c). An SWS of 6–10 m/s was observed between 20°S and 45°S. The directions of wind flow at 20°S–35°S and 35°S–45°S were mainly westward and eastward, respectively. The area after 45°S had an eastward wind flow, with a velocity of >10 m/s. In May and November, the area between 40°S and 50°S showed an eastward wind flow, with a velocity of >10 m/s.

Table 2. Results of Pearson correlation coefficient

Parameters	R-value
SST vs SLP	0.893295
SST vs SWS	−0.8679
SWS vs SLP	−0.70014

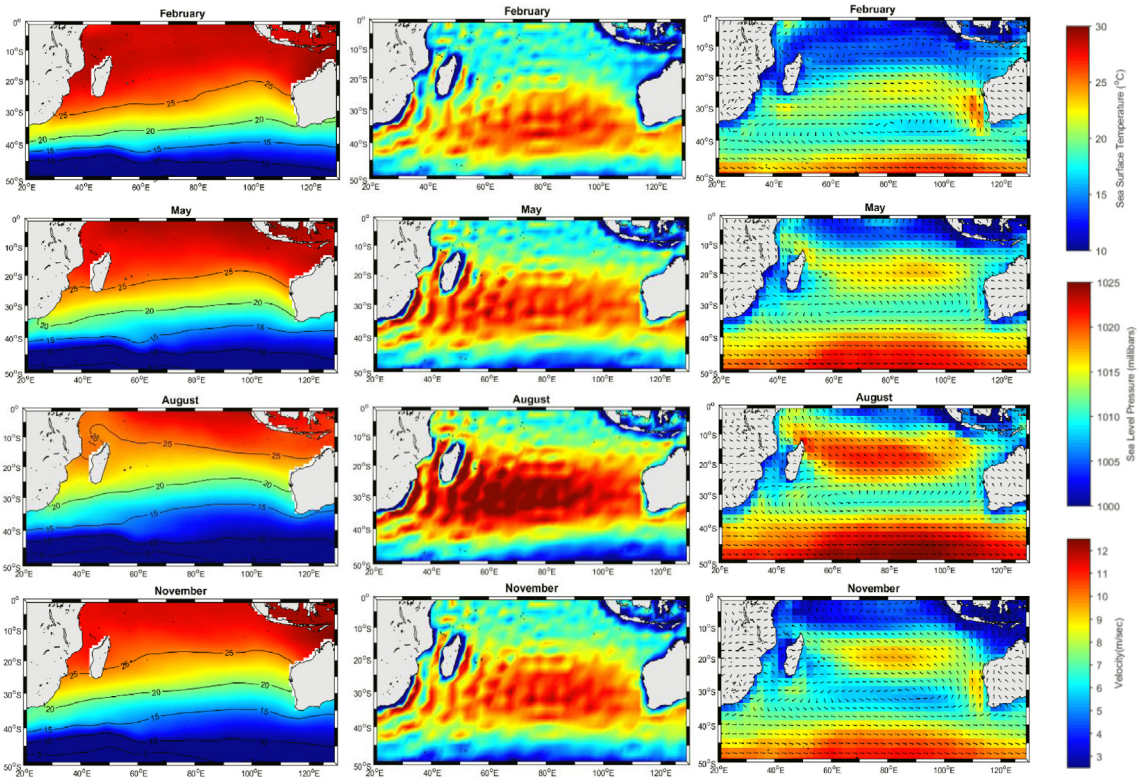

Fig. 4. Mean climatological patterns of (a) SST, (b) SLP, and (c) SWS in February, May, August, and November during 1948−2018.

The wind flow was northward toward the equator from 30°S. During these 2 months, an SWS of 5−10 m/s was observed between 10°S and 40°S. In August, two places showed a high SWS of >10 m/s. The area between 10°S and 20°S and 40°S−50°S with a high SWS showed northwestward and eastward flows, respectively.

3.2. Long-term yearly variation in SST

3.2.1. Time series analysis

Time series of the yearly SST (Fig. 5a) showed that 1948 (blue box) and 2016 (red box) were the coolest and warmest years, respectively, during the study period. From 1948 to 2018, we observed an increasing trend of SST, with a standard deviation of −0.4 to +0.5 (Fig. 5b). After 1969, SST was constant at >21 °C, and up to 2018, it never fell below 21 °C. In 2018, SST crossed 21.8 °C and fell below 21.2 °C. To determine changes in SST every 10 years, a decadal time series was performed. The warmest and coolest decades were 2008−2018 and 1948−1957, with SSTs of 21.46 °C and 20.89 °C, respectively (Fig. 6a) and a standard deviation of 0°−0.18 °C (Fig. 6b). The SST ranges of 1948−1977, 1978−1987, 1988−2007, and 2008−2018 were 20.89°C-21.06 °C, 21.07°C-21.24 °C, 21.25°C-21.44 °C, and 21.45°C-21.46 °C, respectively.

3.2.2. Long-term changes and trends in SST

The long-term SST anomaly changes can effectively determine the exact warming trend in each month of every year. Before 1978, negative SST changes were the highest, but they started showing the opposite result after 1978 (Fig. 7). The year 2016 and decade 2008−2018 were the warmest during the study period (Figs. 5 and 6). Positive SST changes were the maximum in the year 2016 and decade 2008−2018 (Fig. 7). The highest SST anomaly change was observed in March 2016, with a value of >0.6 °C.

The temporal-spatial trend of SIO SST between 1948 and 2018 is shown on different time scales. Changes in SST were in the range of 0°C-1.5 °C, and the area near 40°S and 60°E showed the highest change (Fig. 8c). Areas at 0°S−10°S, 60°E−80°E, 25°S−35°S, and 80°E−120°E showed high changes, with a value of up to 1.3 °C during 1948−2018, and the change in SST was lower in 1948−1972 than in 1973−2018. Fig. 8a and b shows that the change in SST was in the range of 0°C-0.5 °C and 0°C-1°C, respectively. Analysis of seasonal time series showed changes in SST in three periods, namely

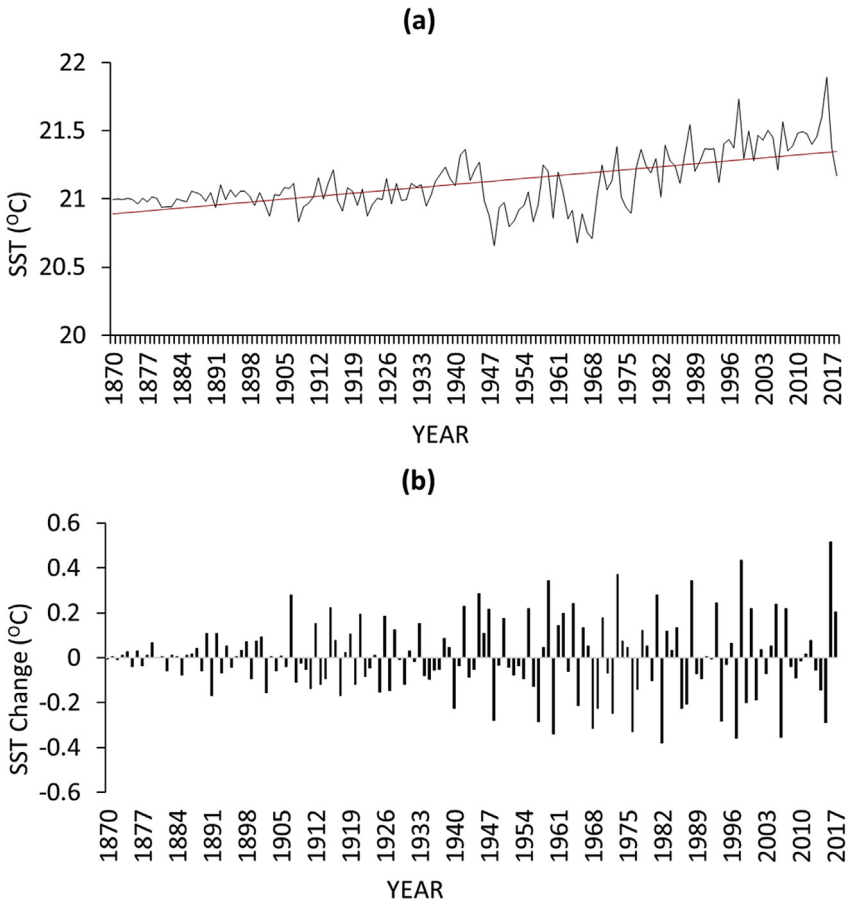

Fig. 5. The time series of (a) yearly SST variation and (b) yearly SST changes during 1948–2018.

1948–1972, 1973–2018, and 1948–2018 (Fig. 9). SST changes during 1948–2018 were much more than those during 1948–1972 and 1973–2018 for all the 4 months. Again, changes during 1973–2018 were more than those during 1948–1972 for all the 4 months. Changes were more in the southwestern part during February, but during May and June, changes were more in the middle part of the SIO for all the three periods. November showed high changes in northwest and eastern Indian Ocean.

4. Discussion

SST is one of the most important environmental factors that hugely contributes to global climate change. Over the past few decades, an increasing trend in temperature has been observed, which has mainly led to global warming. Moreover, SST plays a key role in the distribution of many commercially important fishes. For example, temperate tuna such as albacore prefer approximately 10 °C, but they can stay in warmer water in the subtropical region. Considering the importance of SST with respect to the global scenario, the present study was conducted to determine the interannual, decadal, and seasonal variations of SST in the SIO. Additionally, two important factors, SLP and SWS, were considered to check their role in the SST increase during the study period.

The mean monthly SST showed a negative relation with the mean monthly SWS (Table 2, Fig. 3b) during 1948–2018. The mean monthly SST (Fig. 2a) showed a decreasing trend from January to August, whereas the mean monthly SWS (Fig. 2b) showed an increasing trend during that period. Furthermore, the mean SWS value started decreasing from September, and SST started showing an increasing trend from that month. These results strongly indicate a negative relationship between SWS and SST. The area between 45°S and 50°S had a high wind speed (>12 m/s) throughout all the 4 months (Fig. 4). This area showed an SST of 5°–10 °C in all the 4 months in the entire study period. The area between 0°S and 20°S had a slow SWS (<5 m/s) and a high SST (>25 °C) in all 4 months during the entire study period, except in August. In May, the 25 °C isotherm

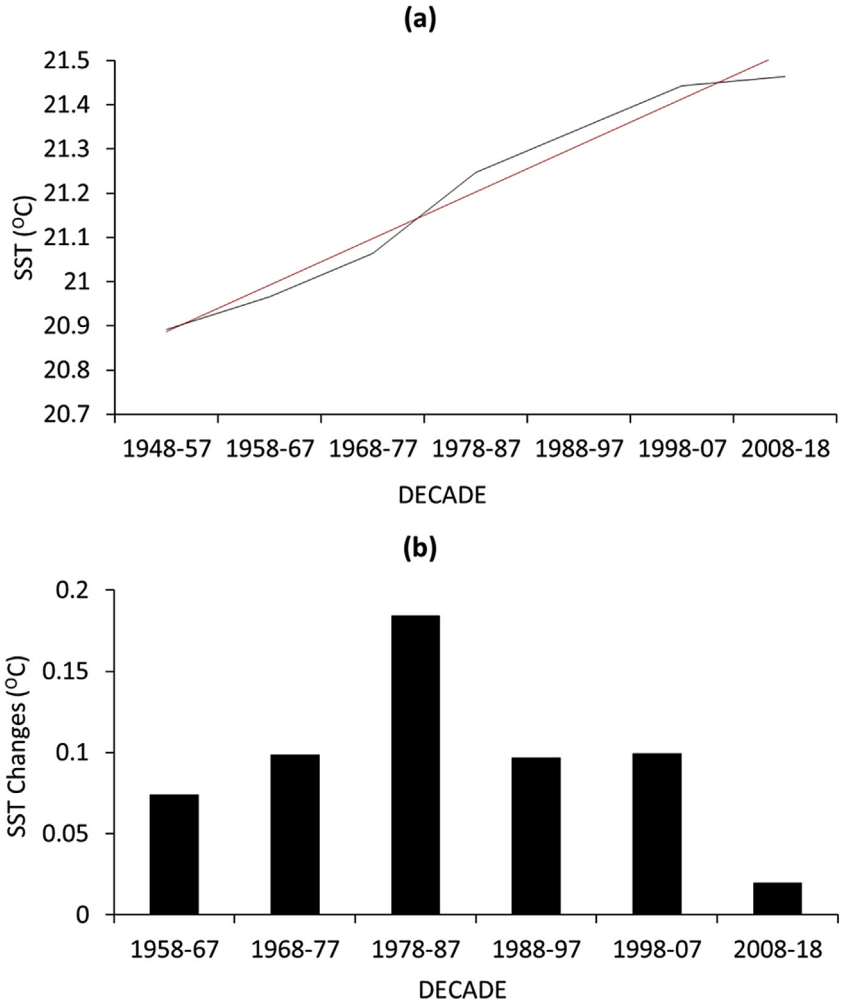

Fig. 6. Time series of (a) decadal SST variation and (b) decadal SST changes during 1948–2018.

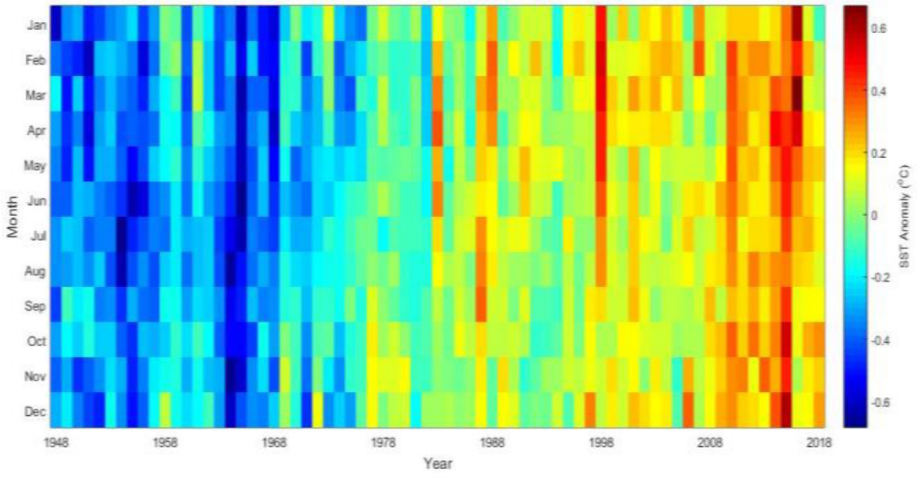

Fig. 7. Long-term changes in SST anomalies during 1948–2018.

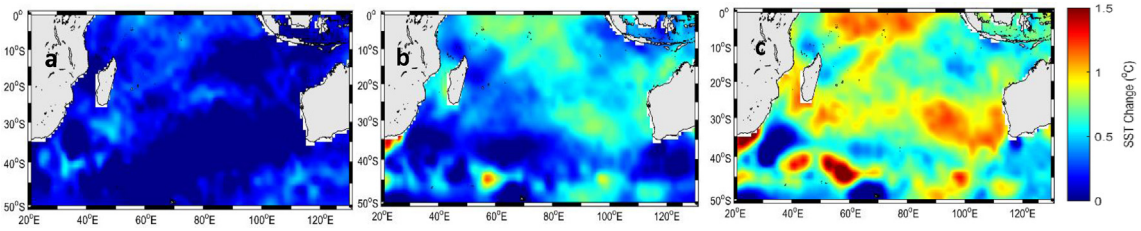

Fig. 8. Temporal-spatial SST trends between 1948 and 2018 on different time scales in the SIO: (a) 1948–1972, (b) 1973–2018, and (c) 1948–2018.

line was near 25°S in the western Indian Ocean, and the mean SWS was 7–9 m/s. However, this line shifted north-westward near 5°S, which implies cooling between 5° and 20°S in August, and the mean SWS of that area was also 10–12 m/s, which was mainly on the northwest in that particular month. These results indicate a negative relationship between SST and SWS during the study period. Moreover, previous studies have shown a negative correlation between SST and SWS [11–16]. The main reason for this negative relation between SST and SWS is the alteration of surface water stratification by the high wind speed, which brings the colder subsurface water to surface, decreasing SST. Another strong potential reason is that a higher wind speed accelerates the evaporation process, which can cause SST cooling. Gabric et al. (2012) stated that a negative relation exists between SST and SWS, and he discussed the low SWS in summer and high SWS in spring and winter (negative correlation). Ng et al. [17] concluded that a high wind speed such as 15 m/s can significantly affect the SST retrieval. Wang et al. [18] discussed the relation between wind speed, evaporation, and SST changes and mentioned that increased evaporation caused by increase in wind speed results in SST cooling, which further can increase the wind speed. However, Xie [19] stated that a positive correlation exists between SST and SWS over a small-scale region. This result differed from that of the present study, which may be due to the study area, study time, and area coverage.

Few studies have discussed the association between SST and SLP, where authors have not elaborated on the type of relationship between two factors. However, studies have tried to evaluate the relationship through statistical analyses. The mean monthly SST showed a positive correlation with the mean monthly SLP (Table 2, Fig. 3a) during 1948–2018. Both SLP and SST showed decreasing and increasing trends from January to August and September to December, respectively. The mean monthly SLP was negatively correlated with the mean monthly SWS. A negative correlation between

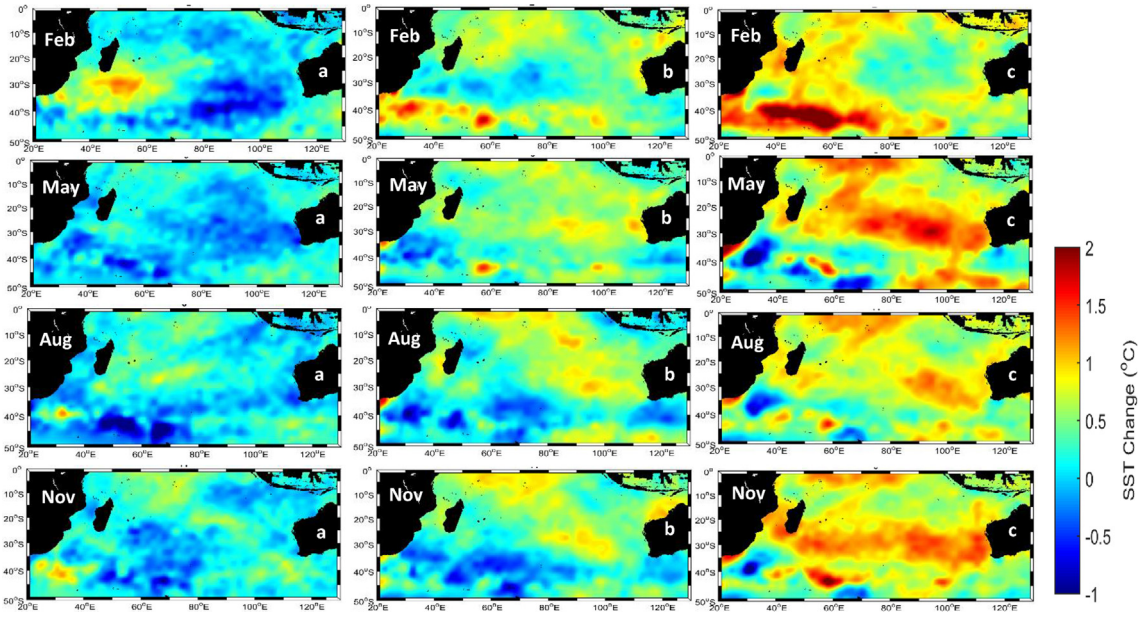

Fig. 9. Seasonal SST changes during (a) 1948–1972, (b) 1973–2018, and (c) 1948–2018 in the SIO.

SLP and SWS can support the positive relationship between SLP and SST, as a negative correlation was found between SST and SWS (Table 2). SST in the range of 10°−25 °C was observed in the area of 0°S−45°S, where the mean monthly SLP was in the range of 1010−1025 millibar. However, the area between 45°S and 50°S had an SST of <10 °C, and this area had a relatively low SLP of <1010 millibar. These results indicate a positive correlation between the mean monthly SST and SLP. Haworth [20] studied the relationship between the mean monthly SST and SLP and stated that the SLP anomaly pattern can cause SST anomalies and then make synchronous contributions to pressure anomaly. Moreover, using the Principle Component Analysis (PCA) analysis, Haylock et al. [21] showed that 40% of SST changes is contributed to by SLP in the north Atlantic Ocean. They hope to further study the relationship between SST and SLP for obtaining a clearer understanding.

The global trend of SST showed tempo-spatial, seasonal, and long-term yearly SST variations. SST changes in February were more than those in other months during the entire study period, as that month is indicated as the start of summer in the SIO. During this time, the southwest Indian Ocean had higher SST changes, especially the south coast of Madagascar, than all other parts of the Indian Ocean. Reason [22] stated that the southwest Indian Ocean is warmer than the southeast Indian Ocean during summer, which causes heavy rainfall in the southeastern African coast. The tempo-spatial SST trend showed that SST changes were more in 1973−2018 than in 1948−1972. The same pattern was followed by long-term yearly SST variations during the study period. Moron et al. [23] described a warming trend in the Indian Ocean and Atlantic Ocean during 1910−1940 and since 1975, respectively. A cooling trend was noted in SST between these two periods. The present study showed that changes in SST were <0.3 °C during 1948−1972 but were in the range of 0°−1.5 °C during 1973−2018. Bichet et al. [24] suggested that during 1950−1970, the greenhouse gas effect was masked by the aerosol emission due to the higher response on aerosol emission than greenhouse gas emission by atmosphere. That might be one reason for cooling during 1948−1972. Furthermore, yearly variation in SST showed an increasing trend from 1948 to 2018. In the present study, a global SST increase of 0.5 °C was noted from 1948 to 2018 (Fig. 5). Bichet et al. [24] noted an SST increase of 0.4 °C from 1930 to 2005. One of the strongest possible reasons for the SST increasing trend is the increasing trend in CO_2 emission. Many previous studies have also discussed the relation between SST and CO_2, which was mainly positive. Greenhouse gases can hugely affect climate variability, which indicate a linear increase in SST and CO_2 [25]. Dutton et al. [26] suggested that changes in SST threshold were due to increased CO_2.

Some studies have discussed the effect of sub-tropical Indian Ocean dipole (SIOD) on SST

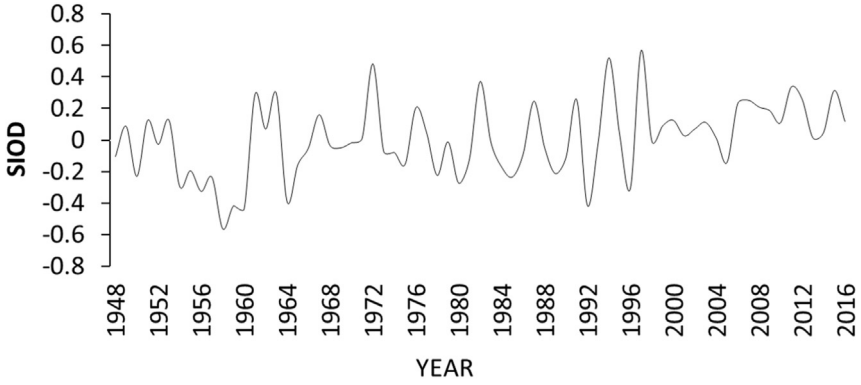

Fig. 10. SIOD events during the study period.

Table 3. Positive and negative SIOD events during the study period.

EVENT	YEAR
Positive	1949, 1951, 1953, 1961, 1962, 1963, 1967, 1971, 1972, 1976, 1977, 1982, 1987, 1991, 1994, 1995, 1997, 1999, 2000, 2001, 2002, 2003, 2004, 2006, 2007, 2008, 2009, 2010, 2011, 2012, 2013, 2014, 2015, 2016
Negative	1948, 1950, 1952, 1954, 1955, 1956, 1957, 1958, 1959, 1960, 1964, 1965, 1966, 1968, 1969, 1970, 1973, 1974, 1975, 1978, 1979, 1980, 1981, 1983, 1984, 1985, 1986, 1988, 1989, 1990, 1992, 1993, 1996, 1998, 2005

changes in the SIO. The index of subtropical dipole is computed by determining the SST anomaly difference between the western (55°−65^0 E, 27°−37°S) and eastern (90−100°E, 18°−28°S) subtropical Indian Ocean [27]. Dipole mode events evolve in the subtropical SIO region during the austral summer [28]. This was linked with the strengthening/weakening of the Mascarene High. Furthermore, the southwest Indian Ocean becomes warmer and the southeast Indian ocean cooler during the positive SIOD event, and the opposite occurs during the negative SIOD events. Several papers have discussed the SIOD impact on regional and global climate variabilities [29−33] and [34].). The subtropical dipole mode in the Indian Ocean is generally found to accompany similar dipole mode events in the subtropical southern Atlantic Ocean [35−37] and Pacific Ocean.

Considering these facts, authors hope to continue this work to determine the relation between SST and SIOD in the SIO more precisely. Long-term variation in SIOD events and number of positive/negative events during the study period are shown in Fig. 10 and Table 3.

Our study on the long-term SST in the SIO provided some crucial insights into SST changes from 1948 to 2018. As mentioned before, SST is related to atmospheric changes and fish habitat. Changes in SST can definitely affect the spatial distribution of any species and atmospheric events. The study results are important because they can provide a clear insight into the changes in the ocean and the reason for the changes.

5. Conclusion

The present study determined the mean monthly variation, and February was observed as the warmest month among all the 4 months studied, and February indicated the start of summer in the Indian Ocean. Long-term yearly time series of SST showed that 2016 and 1948 were the warmest and coolest years, respectively, during the study period. Tempo-spatial changes showed higher changes in SST during 1973−2018 than during 1948−1972. During February, the southwest Indian Ocean was warmer than the southeast Indian Ocean, but during November, the southeast Indian Ocean was warmer than the southwest Indian Ocean. SST showed a strong negative correlation with SWS but a strong positive correlation with SLP. SLP and SWS showed a negative correlation. Spatial distribution showed a high SWS (>12 m/s) near 50°S, with an SST of <10 °C, and areas with a wind speed of <12 m/s showed high SST. Decadal time series showed that 1978−1987 had the highest decade change than all other decades. SST anomalies were almost negative before 1970, positive after 1970, high after 2008, and highest in 2016.

Funding

This research was financed by the Taiwan Council of Agriculture (106AS-10.1.5-FA-F1 (4); 107AS-9.1.5-FA-F1 (4)) and the Ministry of Science and Technology of Taiwan (MOST105-2611-M-019-011).

Declaration of competing interest

The authors declare no conflict of interest

References

[1] McCarthy GD, Haigh ID, Hirschi JJM, Grist JP, Smeed DA. Ocean impact on decadal Atlantic climate variability revealed by sea-level observations. Nature 2015;521(7553):508−10.
[2] https://earthobservatory.nasa.gov
[3] Reynolds RW, Rayner NA, Smith TM, Stokes DC, Wang W. An improved in situ and satellite SST analysis for climate. J Clim 2002;15(13):1609−25.
[4] Cess RD, Potter GL, Blanchet JP, Boer GJ, Del Genio AD, Deque M, et al. Intercomparison and interpretation of climate feedback processes in 19 atmospheric general circulation models. J Geophys Res: Atmospheres 1990;95(D10):16601−15.
[5] Singh OP. Cause-effect relationships between sea surface temperature, precipitation and sea level along the Bangladesh coast. Theor Appl Climatol 2001;68(3−4):233−43.
[6] Khan TMA, Quadir DA, Murty TS, Kabir A, Aktar F, Sarker MA. Relative sea level changes in Maldives and vulnerability of land due to abnormal coastal inundation. Mar Geodes 2002;25(1−2):133−43.
[7] Evan AT, Camargo SJ. A climatology of Arabian Sea cyclonic storms. J Clim 2011;24(1):140−58.
[8] Emanuel KA. The dependence of hurricane intensity on climate. Nature 1987;326(6112):483−5.
[9] Michaels PJ, Knappenberger PC, Davis RE. Sea-surface temperatures and tropical cyclones in the Atlantic basin. Geophys Res Lett 2006;33(9).
[10] Yadav PK, Prajapati NL. An overview of genetic algorithm and modeling. Int J Sci Res Publ 2012;2(9):1−4.
[11] Hurrell JW. Decadal trends in the North Atlantic Oscillation: regional temperatures and precipitation. Science 1995;269(5224):676−9.
[12] Bjerknes J. Atlantic air-sea interaction. Advances in geophysics, vol. 10. Elsevier; 1964. p. 1−82.
[13] Misra K, Puri AK, Shukla AK, Haroon S, Pandey JD. Interaction studies of Guanosine-DMSO-water system. 1997.
[14] Huang C, Qiao F. The relationship between sea surface temperature anomaly and wind energy input in the Pacific Ocean. Prog Nat Sci 2009;19(10):1409−12.
[15] Qu B, Gabric AJ, Zhu JN, Lin DR, Qian F, Zhao M. Correlation between sea surface temperature and wind speed in Greenland Sea and their relationships with NAO variability. Water Sci Eng 2012;5(3):304−15.
[16] Bryan FO, Tomas R, Dennis JM, Chelton DB, Loeb NG, McClean JL. Frontal scale air−sea interaction in high-resolution coupled climate models. J Clim 2010;23(23):6277−91.
[17] Ng HG, MatJafri MZ, Abdulah K, Wong CJ. The effect of wind speed on SST retrival. Proceedings of Aerospace Conference. IEEE; 2009.

[18] Pelejero C, Grimalt JO, Heilig S, Kienast M, Wang L. High-resolution UK 37 temperature reconstructions in the South China Sea over the past 220 kyr. Paleoceanography 1999; 14(2):224−31.
[19] Xie SP, Carton JA. Tropical Atlantic variability: patterns, mechanisms, and impacts. Earth Climate: The Ocean-Atmosphere Interaction, Geophys. Monogr 2004;147:121−42.
[20] Haworth C. Some relationships between sea surface temperature anomalies and surface pressure anomalies. Q J R Meteorol Soc 1978;104(439):131−46.
[21] Haylock MR, Jones PD, Allan RJ, Ansell TJ. Decadal changes in 1870−2004 Northern Hemisphere winter sea level pressure variability and its relationship with surface temperature. J Geophys Res: Atmospheres 2007;112(D11).
[22] Reason CJC. Subtropical Indian Ocean SST dipole events and southern African rainfall. Geophys Res Lett 2001;28(11): 2225−7.
[23] Moron V, Vautard R, Ghil M. Trends, interdecadal and interannual oscillations in global sea-surface temperatures. Clim Dynam 1998;14(7−8):545−69.
[24] Bichet A, Wild M, Folini D, Schär C. Global precipitation response to changing forcings since 1870. Atmos Chem Phys 2011;11(18):9961−70.
[25] Dickinson RE, Cicerone RJ. Future global warming from atmospheric trace gases. Nature 1986;319(6049):109−15.
[26] Dutton JF, Poulsen CJ, Evans JL. The effect of global climate change on the regions of tropical convection in CSM1. Geophys Res Lett 2000;27(19):3049−52.
[27] http://www.jamstec.go.jp/
[28] Behera SK, Yamagata T. Subtropical SST dipole events in the southern Indian Ocean. Geophys Res Lett 2001;28(2): 327−30.
[29] Reason CJC, Hachigonta S, Phaladi RF. Interannual variability in rainy season characteristics over the Limpopo region of southern Africa. Int J Climatol 2005;25:1835−53.
[30] Mapande AT, Reason CJC. Links between rainfall variability on intraseasonal and interannual scales over western Tanzania and regional circulation and SST patterns. Met Atm Phys 2005a;89:215−34.
[31] Mapande AT, Reason CJC. Interannual rainfall variability over western Tanzania. Int J Climatol 2005b;25:1355−68.
[32] Jia XL, Li CY. Dipole oscillation in the Southern Indian Ocean and its impacts on climate. Chin J Geophys 2005;48: 1238−49.
[33] England Matthew H, Ummenhofer Caroline C, Santoso Agus. Interannual rainfall extremes over southwest western Australia linked to Indian ocean climate variability. J Clim 2006;19:1948−69.
[34] Ash KD, Matyas CJ. The influences of ENSO and the subtropical Indian Ocean dipole on tropical cyclone trajectories in the south Indian ocean. Int J Climatol 2012;32(1): 41−56.
[35] Venegas S, Mysak LA, Straub DN. Atmosphere−ocean coupled variability in the South Atlantic. J Clim 1997;10: 2904−20.
[36] Fauchereau N, Trzasaka S, Richard Y, Roucou P, Camberlin P. Sea-surface temperature co-variability in the southern Atlantic and Indian Oceans and its connections with the atmospheric circulation in the Southern Hemisphere. Int J Climatol 2003;23:663−77.
[37] Hermes JC, Reason CJC. Ocean model diagnosis of interannual coevolving SST variability in the south Indian and south Atlantic oceans. J Clim 2005;18:2864−82.